Advances in Water Resources 32 (2009) 975–985

Contents lists available at ScienceDirect

Advances in Water Resources

journal homepage: www.elsevier.com/locate/advwatres

Ability of a dual polarized X-band radar to estimate rainfall

S. Diss [a,*], J. Testud [b], J. Lavabre [a], P. Ribstein [c], E. Moreau [b], J. Parent du Chatelet [d]

[a] Cemagref, Aix en Provence-Equipe Hydrologie Division OHAX 3275 Route Cézanne - CS 40061 13182 AIX EN PROVENCE Cedex 5, France
[b] Novimet, 10-12, avenue de l'Europe, 78140 VELIZY, France
[c] Université P. & M. Curie (Paris VI), UMR 7619 Sisyphe, 4 place Jussieu, Tour 56, Couloir 46-56, 3° étage, 75252 PARIS Cedex 05, France
[d] Météo France, DSO, Centre de Météorologie Radar, Trappes, France

ARTICLE INFO

Article history:
Received 8 February 2008
Received in revised form 15 January 2009
Accepted 20 January 2009
Available online 30 January 2009

Keywords:
Quantitative precipitation estimation
X-band weather radar
Rainfall

ABSTRACT

The aim of this study is to assess rainfall estimates by a dual polarized X-band radar. This study was part of the European project FRAMEA (Flood forecasting using Radar in Alpine and Mediterranean Areas). Two radars were set up near the small town of Collobrières in South Eastern France. The first radar was a dual polarized X-band radar (Hydrix®) associated with a ZPHI® algorithm while the second one was an S-band radar (Météo France). We compared radar rainfall data with measurements obtained by two rain gauge networks (Météo France and Cemagref). During the experiments from February 2006 to June 2007, four significant rainfall events occurred. The accuracy of the rain rate obtained with both S-band and X-band radars decreased significantly beyond 60 km, in particular for the X-band radar. At closer ranges, such as 30–60 km from the radars, the X-band and the S-band radar retrievals showed similar performance with Nash criteria around 0.80 for the X-band radar and 0.75 for the S-band radar. Furthermore, the X-band radar did not require calibration on rainfall records, which tends to make it a useful method to assess rainfall in areas without a rain gauge network.

1. Introduction

Radar technology has been employed to assist weather predictions for over 40 years but its use for operational hydrology is limited to a decade only. Precipitation estimates based on weather radars can be of a great value for flood forecasting [2,21]. However, the performances of hydrological applications are highly dependent on the accuracy of the rainfall estimates on which they are based [6,3]. Although highly advanced technological methods have been applied on weather radar, the accuracy of the rainfall estimates obtained using radar methods is still problematic [9,18]. Some difficulties, as attenuation, ground echoes and biases on the rainfall were encountered, especially in mountainous areas and for intense precipitation events [12]. Before introducing radar data into rainfall-runoff models, it is necessary to estimate the accuracy of the rainfall rates from weather radars [27].

The performances of radars are generally analysed by comparing their data with rain gauge measurements [11]. These comparisons have given rise to many questions [20,15,17]. One of the main problems when comparing radar and rain gauge data is the difference in the spatial representativeness of the measurements [10]. Radar rainfall is measured over an atmospheric volume while rain gauges measure rain intensity close to the ground. Moreover the spatial heterogeneity of the rainfall is partly responsible for the differences between radar and rain gauge estimates [19]. The radar measurements are prone to many uncertainties due to the complexity of the measurement procedure and atmospheric characteristics of rain [32,33]. Rain gauge stations are also subject to errors of their own. Although radar and rain gauge data are difficult to compare, this analysis has to be done to validate of rainfall estimates before using these data in hydrological modelling.

Some authors proposed to evaluate the mean area precipitation from rain gauges and radar measurements [20,31,12]. Another method consisted in locally comparing radar and rain gauge data [32,18]. All these studies showed significant discrepancies in their results. For instance, Brandes et al. [7] established that the radar to gauge ratios were in the range of 0.7–1.9 for point comparisons at even timesteps.

Radar rainfall was also compared to other rainfall radar estimates using a different data processing [4] or a different radar wavelength [1]. In this case, the comparison between rainfall estimates revealed being free of gauge errors and representativeness differences. Radar to radar evaluation also allowed direct comparison between reflectivity profiles and rainfall rates [30,14]. However, for hydrological applications, it was better to carry the comparison on rainfall rates only.

The aim of this study is to asses the quality of the rain rates obtained by a dual polarized X-band radar to be used for operational flood forecasting in the Mediterranean area. We studied

* Corresponding author. Tel.: +33 442669936.
E-mail address: Stephanie.Diss@cemagref.fr (S. Diss).

0309-1708/$ - see front matter © 2009 Elsevier Ltd. All rights reserved.
doi:10.1016/j.advwatres.2009.01.004

two different radar technologies, an S-band radar developed and used by Météo France [16] and a dual polarized X-band radar, Hydrix®, developed by Novimet. The S-band radar is mainly used in areas with particularly high precipitations. Because of its lightness and its shorter wavelength, the X-band radar is fairly inexpensive and flexible to use, whatever the radar site. Its main limitation is the high attenuation of the X-band frequency exerted by rainfall [13]. The Hydrix® radar is associated with the ZPHI® algorithm [29], which corrects the signal attenuation [23] and yields accurate rainfall estimates, as long as the total extinction point is not reached [28].

In the present paper, we will first describe the experimental catchment area, the two X-band and S-band radars and the rainfall events which occurred during the experiment. Then we will study the methodology and the scores used to compare precipitations derived by the radars with that of the rain gauges. Later, we will analyse the outcomes according to different time-steps (from 5 min to 6 h), for different areas (with a distance from the radar ranging from 0 to 120 km) and for various rain intensities.

2. Experimental set up and data

The X-band radar was set up at the experimental catchment area of the "Réal Collobrier", located near the Mediterranean coast, in the Var department (South-Eastern France) in the North-East of Toulon (Fig. 1). The altitudes of the catchment area range from 80 to 780 m, with a mean altitude of 330 m. The catchment area is approximately 70 km^2. The climate is of Mediterranean type with a very marked period of summer dryness, intense precipitation in the autumn, and a rainy spring season [25]. The X-band radar was used in the framework of the FRAMEA European project (Flood forecasting using Radar in Alpine and Mediterranean Areas). We benefited of a relatively dense ground gauge network and a long-time rainfall data record. Two optical disdrometers were set up at Portanière, 8 km west of the X-band weather radar. One of them was a system set up by CETP and the other one was the THIES system used at Météo France (Fig. 2).

2.1. Weather radars

The two weather radar operating in the FRAMEA experiment were the HYDRIX® radar designed by Novimet and the Météo France S-band radar of Collobrière located within an only 4-km range from each other. The HYDRIX® radar is an X-band polarimetric and Doppler radar. Its main characteristics are listed in Table 1. The primary data generated by HYDRIX® radar were processed in real time by the ZPHI® algorithm allowing radar echo classification (ground clutter, sea clutter, clear air, stratiform rain, convective rain, melting hydrometers, snow, hail), correction for the attenuation, retrieval of parameter N_0^* characteristic of the rain drop size distribution, retrieval of the rainfall rate and quality index. The disdrometer allowed the measurement of the rain drop size distribution and therefore permitted a radar reflectivity calibration, associated with the ZPHI® algorithm as described in Le Bouar [23]. The multi-PPI mode permitted, due to the short dwell time, a rise in the generation of surface rain maps within a 2.5-min period. The four elevation angles (from 0.75° to 3°) allowed filling the gaps caused by ground clutter, topographical beam blocking or bright band. The ground clutters are cancelled by applying a threshold on the variability of the reflectivity computed over each pixel of 1 km square. The reflectivity at the various elevations are corrected from the ground clutters, from partial beam filling, from PVR and then combined together using a weighted average. The weight depends on the altitude at which the measurement was taken, the occurrence of partial beam filling and the ground clutter. Each rainfall rate PPI was projected into a 1 km by 1 km Cartesian grid, using Cressman interpolation. The PPI merging consisted of a linear average weighted according to the quality index [22].The merged PPIs were therefore processed to produce 5-min, 1-h and 1-day rain accumulations. The incomplete accumulations were removed from the analysis.

The S-band radar at Collobrières belongs to the ARAMIS network run by Météo France. The S-band radar also operates at various elevation angles (from 0.4° to 3.6°) but with a time cycle of 5 min. From the measured reflectivity, the instantaneous rainfall rate is computed using the Z–R relationship adjusted in real time by a dynamical calibration based on the Météo France gauge net-

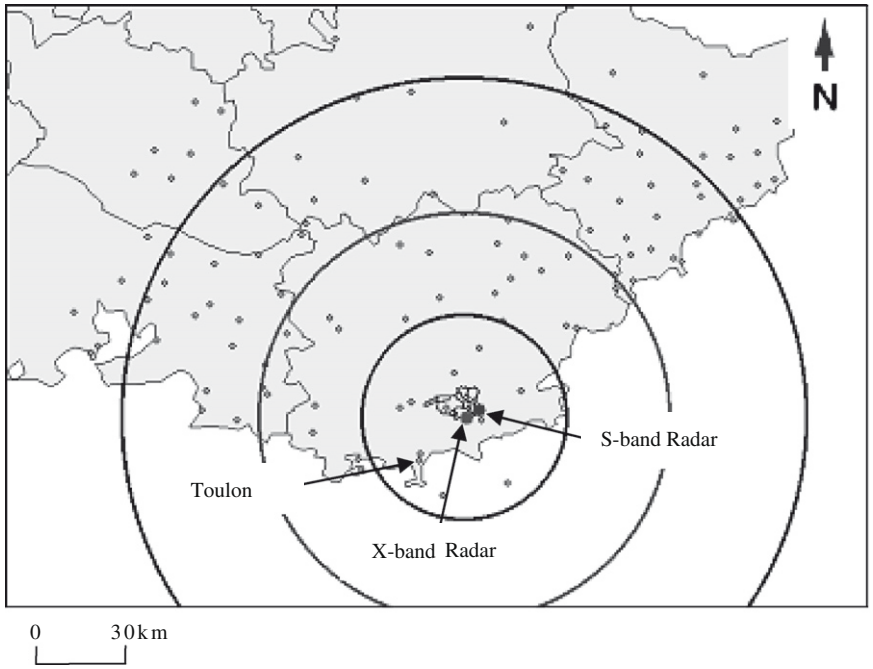

Fig. 1. The localisation of the Météo France rain gauges. The circles delineate the 30, 60 and 100 km radiuses around the X-band radar.

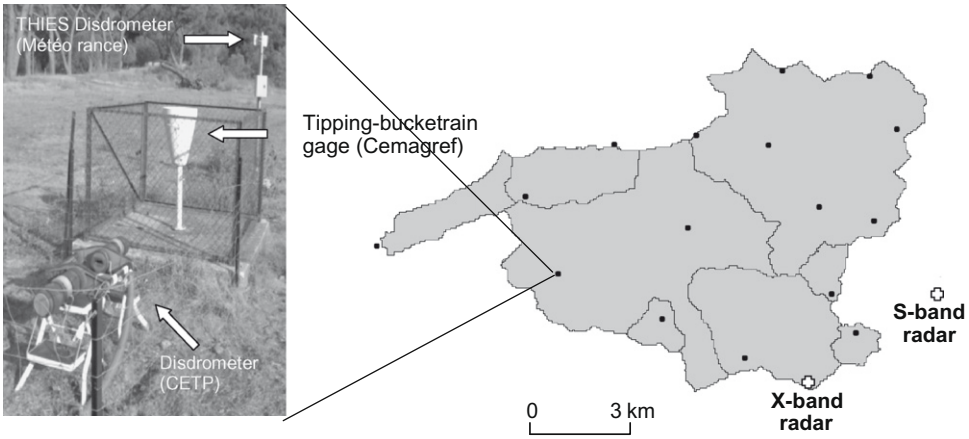

Fig. 2. Réal Collobrier catchment. The rain gauge network (•), the S-band Radar of Météo France (*S*), the X-band radar, Hydrix® (*X*), and the two optical disdrometers.

Table 1
X-band radar (Hydrix®) and S-band radar (Météo France) characteristics. The various parameters measured were: Z reflectivity, V_D Doppler velocity, σ_V spectral width, Z_{DR} differential reflectivity, Φ_{DP} differential phase and ρ_{HV} copolar correlation coefficient.

	S-band radar at Collobrières	X-band radar (HYDRIX®) at Collobrières
Frequency	3 GHz	9.3 GHz
Antenna type	Central feed	Offset
Antenna diameter	5.5 m	1.5 m
Beam aperture	1.2° (3 dB one-way)	1.5° (3 dB one-way)
Side lobes	<25 dB	<30 dB
Radome	Yes, with classical architecture	No
Detection threshold	0 dB to 70 km	0 dB to 70 km
Measured parameter	Z, V_D, σ_v	$Z, Z_{DR}, \Phi_{DP}, \rho_{HV}, V_D\sigma_V$
Technology		HV simultaneously transmitted
Times step	5 min	2 min 30
Altitude	653 m	580 m
Scanning elevation	0.4°; 1.4°; 2.2°; 3.6°	0.75°; 1.5°; 2.25°, 3.0°
Rainfall calculation	Marshall Palmer law + adjustment with rain gauge data	ZPHI software

work [24]. It is a spatially uniform calibration, based on real time rain gauges measurements. The calibration coefficient, updated every hour, is defined as the ratio of hours between accumulated precipitations by rain gauges and radar co-located pixels.

2.2. Rain gauges network

The first gauge network consists of 17 rain gauge stations located in the "Réal Collobrier" catchment area and operated by Cemagref. The second network, operated by Météo France, has more than 100 rain gauge stations spread over a large area in the South of France. Fig. 1 shows the layout of these networks. The temporal resolution for rainfall measurements is respectively 5-min for the first and 6-min for the second network. Both networks are composed of tipping bucket rain gauge stations.

The two networks together allowed to analyse the accuracy of the radar measurements at different ranges: the Cemagref network at a closer range (<10 km) and the Météo France network at a range of up to 120 km. The number of available rain gauges is presented in Table 2 according to the distance from HYDRIX® radar.

Table 2
Available rain gauges network.

Rain gauge network	Distance to HYDRIX® radar	Number of stations
Cemagref network	0–10 km	17
Météo France network	0–30 km	12
	30–60 km	22
	60–120 km	70

2.3. Events

The HYDRIX® radar was operated from February 2006 to June 2007. The daily rain accumulation over the area defined by radar coverage within a 120-km range was used as index. Only the surface was selected, where rain gauge stations were available. The heaviest rainy episodes over this period were selected based on the daily rain accumulations given by the S-band radar. A minimum threshold value of 0.33 mm of mean day accumulation on each pixel and the research of significant flood events in this study area were used to select the heaviest rainy days. Four events, presented in Table 3, were thus selected.

The event of September 14–15, 2006 was characterized by several rainy cells over the cities of Aix en Provence/Marseille and Draguignan/Frejus. The maximum rainfall recorded during this episode was 45 mm in 1 h near Draguignan city. This event was a not stationary convective rainy cell.

The rainy event at Toulon on September 24–25, 2006 exhibited the most intense and localised pattern with a maximum rainfall

Table 3
Selected rain events measured in terms of the maximum rainfall estimated by S-band weather radar.

From day	Today	Month	Year	Maximum intensity (mm/h in 5 min)	Mean rain on each pixel (mm in 1 day)
14	15	9	2006	366.2	20.60
24	25	9	2006	184.2	18.72
18	21	10	2006	190.4	16.94
2	3	12	2006	160.4	10.38

rate of an order of 100 mm in 1 h. This rainy event is identified as a stationary convective storm. Toulon city was subject to sudden strong downpours in the town centre and neighbouring suburbs.

The October 18–21, 2006 event was characterized by a highly widespread rainfall (including the entire Mediterranean basin) associated with the rainfall rate up to 25 mm in 1 h. The long duration of this stratiform event (nearly 4 days) has provided many data points for our comparison and analysis.

During the December 2–3, 2006 event, which occurred nearby the cities of Draguignan/Frejus, the maximum 1-h rain accumulation reached 50 mm. This event was characterized as a not stationary convective rainy cell. The localisation was not the same but the phenomenon was similar to 14–15 September event. This event was very intense and highly localised, producing heavy downpours and floods.

The four selected events are typical of the Mediterranean climate in autumn with a wide spectrum of precipitation rates. A sufficiently large number of data were collected on these events, enabling us to carry out our analysis in good conditions.

3. Methodology

First of all, a critical analysis was conducted on the rain gauge data. Then an interpolation scheme was applied on the pixels of the radars at the locations of the rain gauges. This step was useful to ensure that the radar data were collected at the same location as the rain gauges. Statistical criteria commonly used in hydrology were then computed to assess the overall quality of the radar data.

3.1. Rain gauge data quality

The quality of the rain gauge data depends on the integration time step and the rainfall intensity. It has been observed that the smallest timescales indulge the largest errors in quality measurement. For example, at light to moderate rainfall intensities of up to 5 mm/h, Ciach [8] reported a relative instrumental error of about 7% for the timescale of 5-min, but of only 3% for the hourly timescale. The representativeness error, function of rain intensity and of the integration timescale, is also linked to the spatial correlation of the rainfall. Ciach and Krajewski [9] found that the gauge representativeness error decreases rapidly with accumulation time, the ratio of the gauge error variance to the total radar-gauge difference variance is in the order of 70% (and 20%) for 5 min (and 1 day) accumulation time.

A critical analysis was carried out on the rain gauge data to identify a possible failure (blocked bucket, obstruction by plants or animals...). For this purpose, a filtering procedure was carried out, based on the daily rainfall accumulation from both radars and from the rain gauge stations. First, the relative differences between the rainfall radar and gauge data were computed on a daily basis. When this difference was greater than 50was listed as a possible failure. However, the problem could also be attributed to the radar data. Therefore, the rain gauge stations thus listed were then checked one by one. Three cases were observed: (1) either the 5-min rain gauge data were always zero; (2) or the 5-min rain gauge data were constant during all the day and finally, (3) the rain gauge data were either largely underestimated or overestimated compared to the radar data. In the first two cases, the results of these stations were removed from the comparison. In the last one, the data were kept in the analysis.

3.2. Location of rainfall measurement points

As mentioned in the introduction, the rain gauge data were to be used as the reference data, and therefore, they were assumed to reflect the "reality". We analysed the rain rate error due to the geographical difference between the centre of 1 km square radar pixels and the locations of the rain gauge stations. Three different interpolation schemes of the radar data (the nearest pixel, the average of the 4 nearest pixels and the distance weighted average of the 4 nearest pixels) had been tested on the event of September 24–25, 2006. No significant differences were found on the hourly rain accumulations when compared to rain gauge accumulations (results not shown). The interpolation used in this study was based on the average rainfall of the four pixels closest to the rain gauge station.

3.3. Statistical analysis

To estimate the overall accuracy of the radar data, we used the Nash criterion and the coefficient of determination (R^2 where R represents the linear correlation coefficient), commonly used in hydrology.

The Nash criterion (Eq. (1)) characterizes the dispersion of the points around the $x = y$ bisect, it can vary from $-\infty$ to 1. The optimal value is 1.

$$\text{Nash} = 1 - \frac{\sum_{i=1}^{n}(x_i - y_i)^2}{\sum_{i=1}^{n}(y_i - \bar{y})^2} \quad (1)$$

In Eq. (1), x denotes the estimated value (i.e., the radar estimated rainfall); y denotes the reference value (i.e., the rain gauge measured data), $\bar{y}$ represents the average reference value and n corresponds to the total number of data points.

The coefficient of determination (R^2) characterizes the dispersion of the points around the linear regression line $y = ax + b$. The R^2 values are between 0 and 1. The radar rainfall estimates are more satisfactory as this coefficient tends to 1.

When the Nash criterion is close to unity, it implies a similar value for the coefficient of determination: a sufficiently high value of the latter could be associated with a very low Nash criterion value. This could imply for example, a systematic bias in the results as discussed in the next section in more details. The two criteria are therefore complementary. Additionally, we used the orthogonal fit which is characterized by the slope and the offset. This statistical criterion allows having quantitative information on this bias.

4. Results

The flood events typically observed in the Mediterranean area are flash floods, i.e., a rapid flooding caused by intense precipitations. Our hydrologic purpose is to work with river basins of more than 10 km^2 with an extremely high spatial variability of the rainfall. The time response of such basins could be as small as few tens of minutes [12]. However, for operational hydrology, models like GR for example, used 1-h or 1-day rain accumulation information as input.

At first, we will describe the influence of the accumulation time (from 5 min to 6 h) on the radar-gauge comparison. Next the observations of the influence of the distance from the radar, based on 1-h rain accumulation, will be detailed. Finally, we shall analyse the influence of rainfall thresholds on the criteria values.

4.1. Accumulation time

The minimum accumulation time available with both radars is 5 min. The rain gauge data with 5-min timescale were only recorded by the Cemagref gauge network located in the "Réal Collobrier" catchment area. The strongest rainfall episode over this catchment was observed from 18 to 21 October, 2006. Fig. 3 shows the Nash criteria of the radar-gauge comparison for this event at

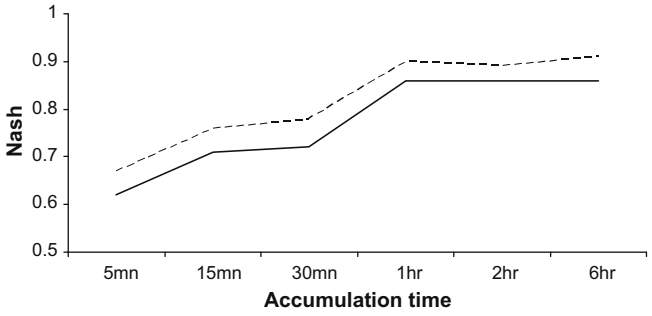

Fig. 3. Nash Criteria obtained by comparison between rain gauge rainfall rates (mm) and the rain rates estimated by X-band and S-band weather radars (mm) with different accumulation times in the range of 10 km around the radars for the October 18–21, 2006 event. The line represents the results of X-band radar and the dotted line shows the results for S-band radar.

different timescales (5 min, 15 min, 30 min, 1 h, 2 h and 6 h). The 5-min timescale comparison is characterized by a large dispersion with Nash criterion of 0.64 for the Hydrix® X-band radar and of 0.69 for the Météo France S-band radar (Table 4). With the increase of the timescale from 5 min to 1 h, we observed an increase of the Nash criteria up to 0.86 for the X-band radar and 0.90 for the S-band radar. On an 1–6 h timescale, the Nash criteria stay relatively constant. A similar behaviour was observed for the coefficient of determination. These results are due to several factors: greater instrumental errors at 5-min than at 1-h timescale; the representativeness errors of the gauges compared to the 1 km square radar pixels; the representativeness errors of the radar for measurements in altitude; a possible time shift in the two datasets.

To minimize the problem of time co-localisation, the rain data at 5-min timescale were compared in terms of distribution function (see Fig. 4). This figure demonstrates that radar and rain gauge rain rates have rather similar distributions up to the rain rate of 3 mm per 5 min. In fact, three classes of the rain rate regime could be distinguished. The first one is for the low rainfall (<1 mm per 5 min), when the S-band radar and the rain gauge have very close distributions, whereas the X-band radar tends to underestimate this class. For the moderate rainfall (from 1 mm to 3 mm per 5 min), the X-band data equal the rain gauge distribution and the S-band radar starts to underestimate the rainfall of this class. Both radars tend to underestimate the high rainfall (>3 mm per 5 min), with an obviously stronger underestimation by the S-band radar.

Theses results brought us to a preliminary conclusion that a 5-min rain rate is subject to more uncertainties compared to an hourly rain rate. Therefore, only hourly accumulations were considered in our next tests.

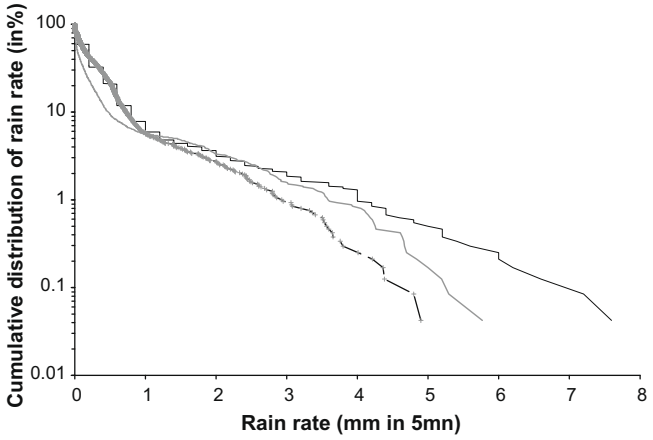

Fig. 4. Distribution of 5-mn rainfall levels on October 18–21, 2006. The black line represents the rain gauges data. The grey line refers to the X-band radar data. The grey line with crosses shows the S-band radar data.

4.2. Distance from the radar

4.2.1. Distance limits

One of the aims of our study was to point out whether the distance from the radar could have an effect on the rainfall estimation.

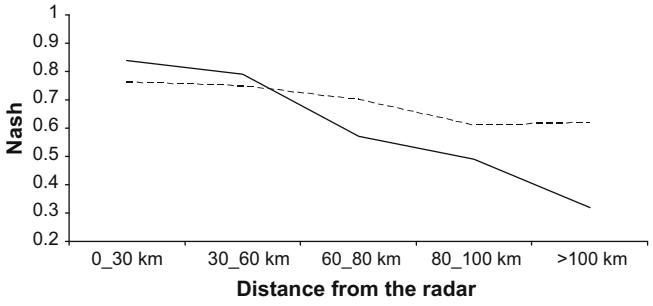

Fig. 5. Nash Criteria obtained by comparison between rain gauge rainfall rates (mm) and the rain rates estimated by X-band and S-band weather radars (mm) with different ranges around the radars for the four events. The line represents the results of X-band radar and the dotted line shows the results for S-band radar.

Table 4
Statistical criteria for 5 min to 6 h comparisons between the data recorded on October 18–21, 2006 event within a range of 10 km from the radars. Nash GX, Nash GS and Nash SX are the Nash criteria between X-band radar and gauge data, S-band radar and gauge data and X-band and S-band radar data, respectively. R^2GX, R^2GS and R^2XS are the determination coefficients between X-band radar and gauge data, S-band radar and gauges data and X-band and S-band radar data, respectively. The regression slopes and offsets are the coefficients of the orthogonal regression lines.

Accumulation time	5 min	15 min	30 min	1 h	2 h	6 h
Nash GX	0.64	0.71	0.72	0.86	0.86	0.86
Nash GS	0.69	0.76	0.78	0.90	0.89	0.91
Nash SX	0.57	0.73	0.76	0.82	0.81	0.81
R^2 GX	0.66	0.75	0.77	0.88	0.89	0.91
R^2 GS	0.68	0.78	0.80	0.90	0.89	0.92
R^2 SX	0.71	0.83	0.87	0.88	0.86	0.85
Slope GX	0.93	0.93	0.93	1.06	1.07	1.00
Slope GS	0.83	0.80	0.78	0.92	0.94	0.97
Offset GX (mm/h)	0.09	−1.22	−1.24	−0.43	−0.45	−0.35
Offset GS (mm/h)	0.03	0.38	0.47	0.11	0.08	−0.03
Number of points ⩾ 0 mm	2415	805	402	239	119	39

Table 5
Statistical criteria for hourly comparisons between the data recorded on all the events within a range of 0 to 60 km from the radars. The various statistical criteria presented in this table are explained in Table 4.

Events	14–15/09/2006	24–25/09/2006	18–21/10/2006	02–03/12/2006	All
Nash GX	0.75	0.85	0.84	0.75	**0.79**
Nash GS	0.66	0.74	0.89	0.80	**0.76**
Nash SX	0.75	0.53	0.81	0.68	0.71
R^2 GX	0.76	0.86	0.86	0.78	**0.80**
R^2 GS	0.71	0.75	0.89	0.81	**0.76**
R^2 SX	0.77	0.76	0.87	0.71	0.74
Slope GX	0.92	1.00	1.03	0.81	**0.94**
Slope GS	1.05	0.82	0.92	0.85	**0.91**
Offset GX (mm/h)	−0.26	−0.01	−0.20	−0.15	−0.16
Offset GS (mm/h)	0.05	0.18	0.03	0.15	0.09
Number of points ⩾ 0 mm	781	963	629	883	**3256**
Number of points ⩾0.1 mm	532	599	478	663	**2272**

The radar-rain gauge comparison was first analysed within different ranges around the radars (Fig. 5). Hourly accumulations were considered in the following description.

From 0 to 30 km and from 30 to 60 km around the radars the statistical results were the same, with Nash criteria around 0.8 for the X-band radar and around 0.75 for the S-band radar. Beyond a range of 60 km around the radars, the Nash criteria decreased for both radars, especially for the X-band radar. For a range between 80 and 100 km around the radars, the Nash criteria are 0.5 for the X-band radar and 0.6 for the S-band one. The determination coefficients showed similar decreases beyond a 60-km radius. It was shown, that the score (in terms of Nash coefficient) was almost constant up to 60 km and then decreased significantly for the X-band radar. The score is lower for the S-band at a short range (up to 60 km), but remains quite stable at a longer one (Fig. 5). These results showed that the range limit for the X-band radar is about 60 km. The differences observed in the range limit could be explained by a higher attenuation by melting particles more pronounced at X-band than at S-band.

Our next step was to analyse the accuracy of the rainfall estimates by radars within a maximum range of 60 km.

4.2.2. Within the 60-km range

In order to study the validity range of the X-band radar within a 0–60 km range, we used 34 rain gauges.

The comparison between S-band and X-band radars showed fairly similar results in general, using the rain gauge rate as references. Combining all the events, Nash criterion and the coefficient of determination were both 0.76 for the S-band radar and 0.79 and 0.80 for the X-band radar (Table 5). The statistical criteria were mostly in favour of the X-band radar, except for the October event.

We observed a few differences between the various events in terms of Nash and coefficient of determination. For example, on September 14–15, a relative large dispersion was observed for both radars (Figs. 6 and 7) when compared to the rain gauges data. Whereas, for September 24–25 event, the radars and rain gauges measurements showed consistency. For the December 2–3 event, the slope of the orthogonal fit is relatively low (around 0.8) for

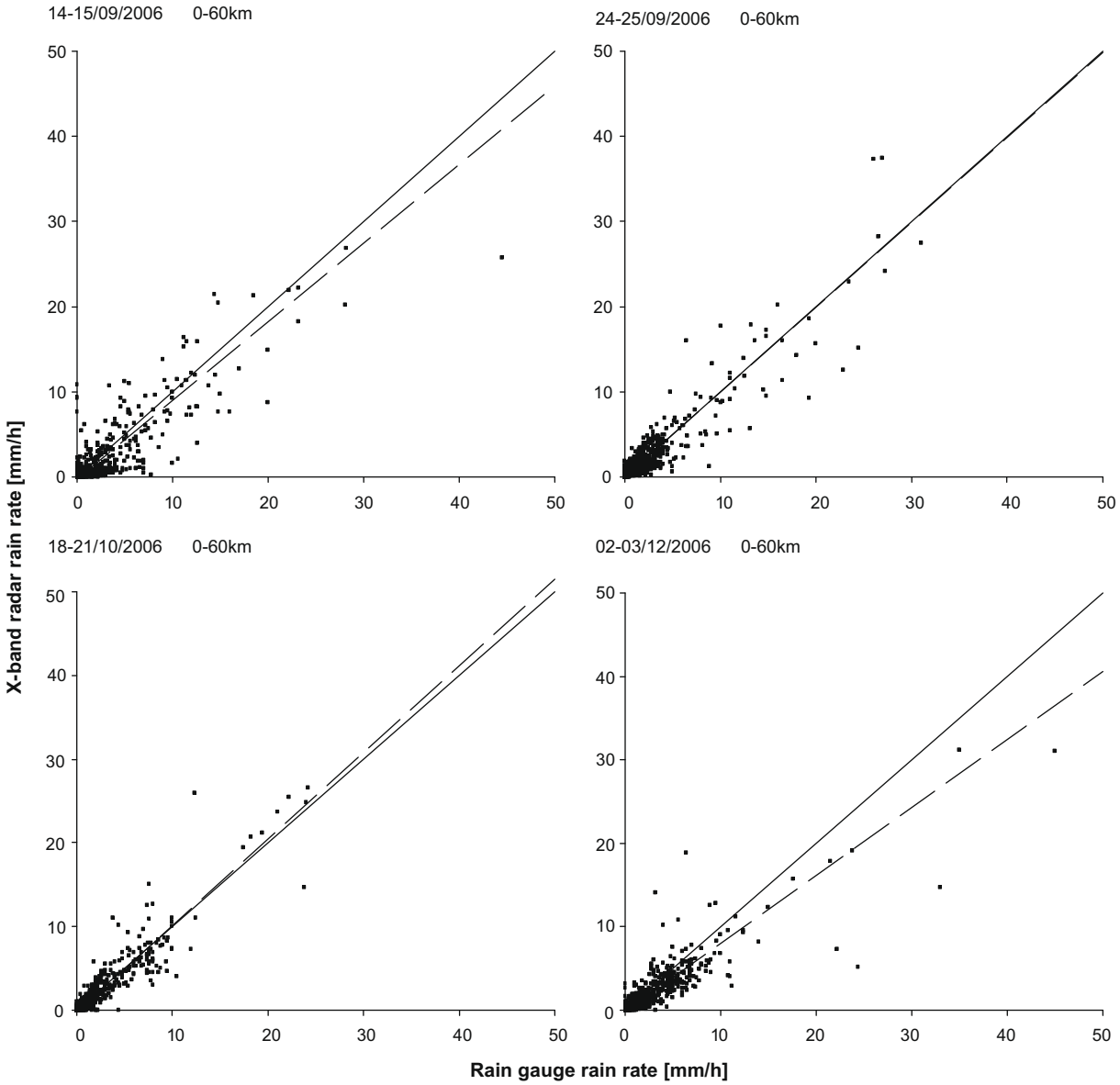

Fig. 6. Scatterplots of hourly rain gauge rainfall rates (mm/h) vs. the hourly rain rates obtained by X-band radar weather radar (mm/h) in 60 km range around the radars for the four events. The dotted line refers to the regression line.

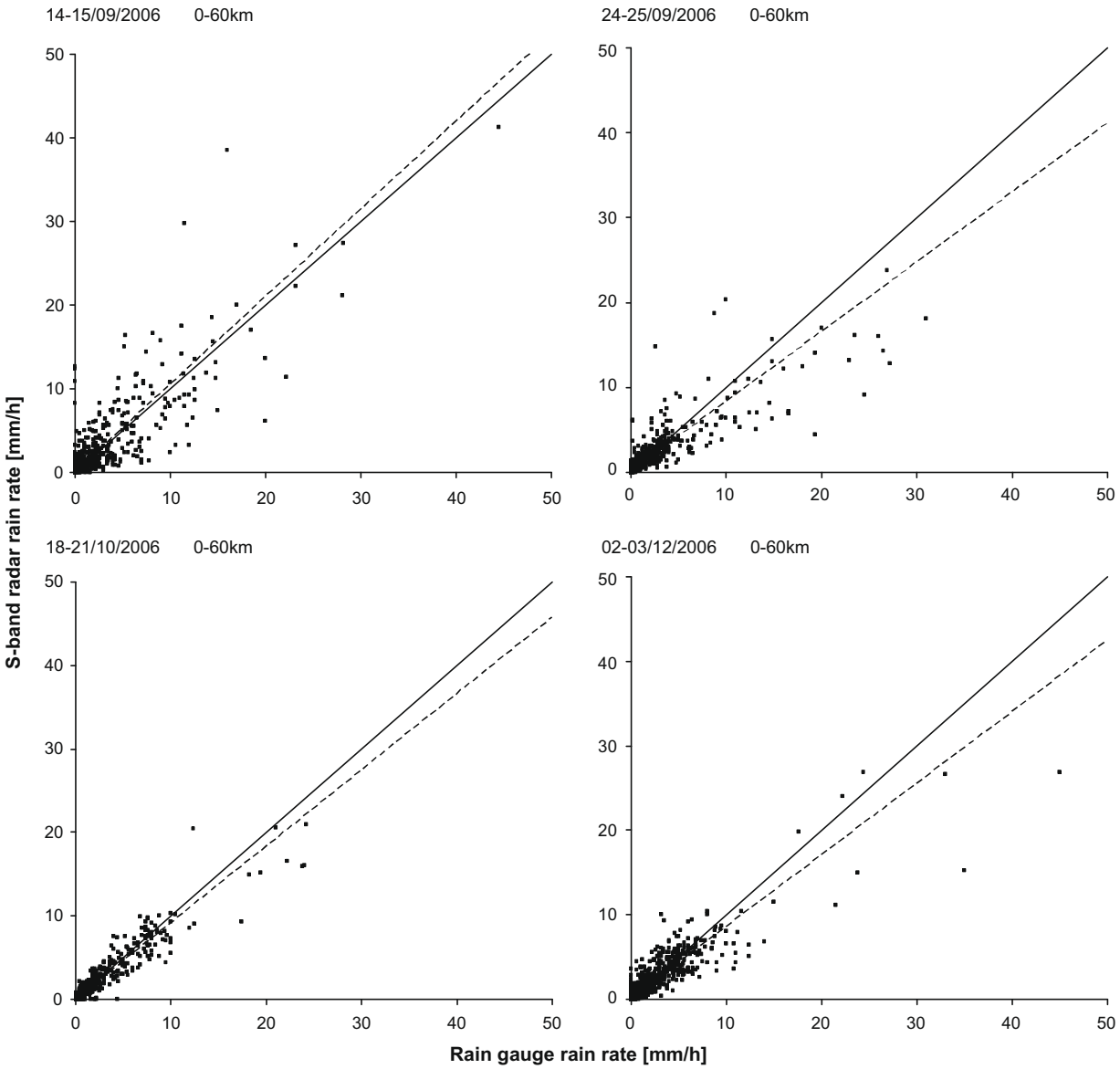

Fig. 7. Scatterplots of hourly rain gauge rainfall rates (mm/h) vs. the hourly rain rates obtained by S-band radar weather radar (mm/h) in 60 km range around the radars for the four events. The dotted line refers to the regression line.

both radars. The highest rain gauge measurements (up to 30 mm/h) are underestimated by both radars. S-band reflectivity is only marginally affected by rain attenuation and the underestimation is not directly linked to the attenuation correction of the X-band radar. The high rainfall intensity occurred within the range of 30–60 km. The underestimated results could be explained by the volume size of the radar beam, which was similar for both radars.

In Table 5, we pointed out that for the Nash criteria between the S-band and X-band radars (noted as Nash-SX) are lower than those computed between either the S-band radar or the X-band radar and the rain gauge, for the most of the events. Fig. 8 presents scatterplots of hourly rainfall derived from both radars, for the four events. The lowest rainfall (<10 mm/h) show constant results whereas for the high rainfall (>10 mm/h) large differences appeared depending on the event. For the September 14–15 event, the S-band radar overestimated the high rainfall compared to the X-band radar, whereas the opposite was observed for the September 24–25 and October 18–21 events. So on the Nash criterion is thus biased and the coefficient of determination (R^2-SX) is greater than that between the radars and the rain gauges.

The reason that both radars did not have the same wavelength was not a suitable explanation. This difference resulting from the radar to radar comparison could be explained by the fact that two different data processings were used during the observations.

4.2.3. Within the 30-km range

The increase of the volume size and the height of radar measurements according to the distance have an influence on the radar-rain gauge comparison. To estimate this impact, we limited the comparison within a range of 30-km radius around the radars. Table 6 summarized the statistical criteria computed for each event and when combining all events. For the second case, the Nash criterion and the coefficient of determination were 0.76 and 0.77, respectively, for the S-band radar and 0.80 and 0.82 for the X-band radar. We also observed variability from one event to another, with a Nash criteria range of 0.54–0.89 for the S-band radar, for example. The September 14–15 event exhibited a relatively low Nash criteria range. This event also demonstrated a better correlation between the two radars rather than between the radars and

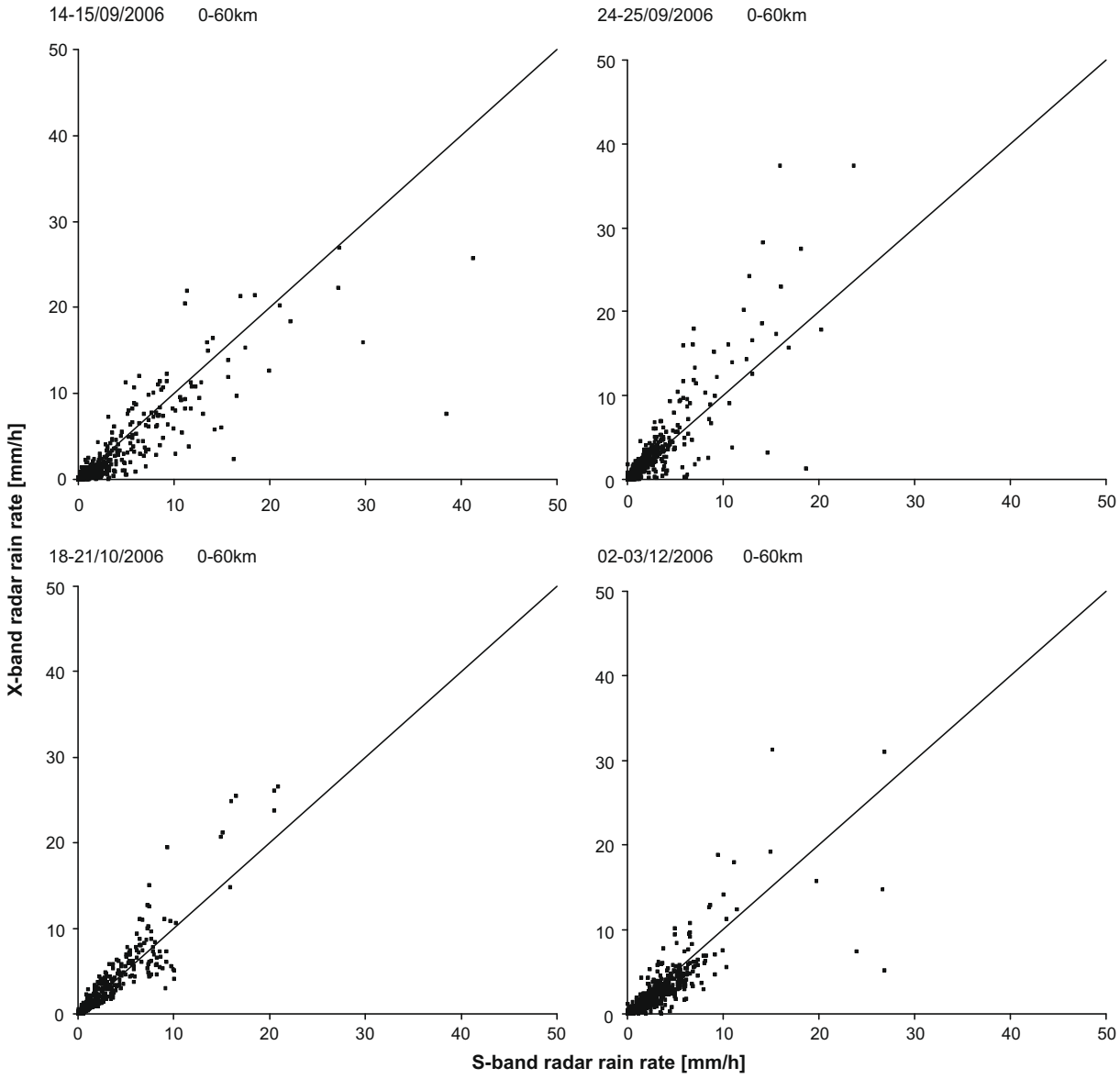

Fig. 8. Scatterplots of hourly S-band radar rain rates (mm/h) vs. the hourly rain rates obtained by X-band radar weather radar (mm/h) in 60 km range around the radars for the four events.

Table 6
Statistical criteria for hourly comparisons including all events within a range of 0–30 km from the radars. The statistical criteria presented in this table are explained in Table 4.

Events	14–15/09/2006	24–25/09/2006	18–21/10/2006	02–03/12/2006	All
Nash GX	0.71	0.79	0.87	0.75	**0.80**
Nash GS	0.60	0.54	0.89	0.82	**0.76**
Nash SX	0.76	0.66	0.83	0.77	0.78
R^2 GX	0.74	0.81	0.88	0.82	**0.82**
R^2 GS	0.69	0.67	0.90	0.82	**0.77**
R^2 SX	0.81	0.69	0.88	0.84	0.80
Slope GX	0.93	1.00	1.02	0.82	**0.96**
Slope GS	1.10	1.08	0.90	0.95	**1.00**
Offset GX (mm/h)	−0.39	−0.05	−0.33	−0.21	−0.25
Offset GS (mm/h)	0.01	0.14	0.09	0.08	0.09
Number of points $\geqslant$ 0 mm	447	566	372	485	**1870**

gauges, indicating a large representativeness error coming from the rain gauges for this particular event.

Compared to the results obtained within the 60-km range, the S-band and X-band radars presented very stable performances, with a constant Nash criterion of around 0.76 and 0.80, respectively. Similar tendencies were observed for the coefficient of determination. The slope of the regression fit was closer to one within the 30-km range for both radars.

In all the events, a better correlation between the two radars was observed in the 30-km range compared to that within the 60-km range (R^2-SX of 0.74 and 0.80). Indeed, in the first case, the relative bias between the two radars was reduced, in particular for the September 24–25 event.

4.2.4. At close range

This analysis took advantage of the small and dense "Réal Collobrier" gauge network, neighbouring both radars by less than 10 km. The interest of focusing on such close range remains in the fact that errors in this case are relatively low (e.g. representativeness error, attenuation or partial beam blocking issues...). Moreover, the rain gauges in this area were not taken into account in the calibration of the S-band radar.

Table 7
Statistical criteria for hourly comparisons including all events within a range of 0–10 km from the radars. The statistical criteria presented in this table are explained in Table 4.

Events	14–15/09/2006	24–25/09/2006	18–21/10/2006	02–03/12/2006	All
Nash GX	0.57	0.85	0.86	0.75	**0.78**
Nash GS	0.49	0.53	0.90	0.84	**0.76**
Nash SX	0.75	0.64	0.82	0.75	0.77
R^2 GX	0.63	0.87	0.88	0.83	**0.80**
R^2 GS	0.65	0.69	0.90	0.84	**0.78**
R^2 SX	0.82	0.70	0.88	0.86	0.80
Slope GX	0.94	0.91	1.06	0.81	**0.97**
Slope GS	1.16	1.10	0.92	0.98	**1.01**
Offset GX (mm/h)	−0.46	−0.06	−0.42	−0.21	−0.31
Offset GS (mm/h)	−0.08	0.19	0.11	0.11	0.11
Number of points ⩾0 mm	320	378	239	339	1276

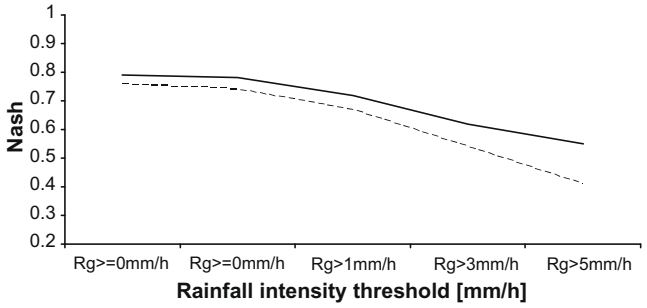

Fig. 9. Nash Criteria obtained by comparison between rain gauge rainfall rates (mm) and the rain rates estimated by X-band and S-band weather radars (mm) with different intensity rainfall threshold for the four events. The line represents the results of X-band radar and the dotted line shows the results for S-band radar.

From the whole set of events (last column of Table 7), the three comparisons (i.e., gauge vs. X-band, gauge vs. S-band and X-band vs. S-band) have very similar Nash criteria (∼0.77) and determination correlations (∼0.80). Additionally, from both radar vs. gauge regressions, the slopes are satisfyingly close to unity (although a slight underestimation by the X-band radar was noted), while the offsets are quite negligible.

In contrast with the overall satisfying correlations mentioned above, the Nash criteria for radar vs. gauge plots differ significantly from one event to another, ranging from 0.49 to 0.90 for the S-band radar, and from 0.57 to 0.86 for the X-band radar. The fact that this variability is weaker for the X-band radar may be assigned to the capability of ZPHI® to automatically adapt the Z–R relationship to the natural variability of the rain, thus exhibiting less contrasted performances than for the S-band radar.

The worst correlations were observed for the September 14–15 event. The reference time shift, manually checked, has been excluded from the possible reasons for this. Since the correlation between both radar data is much better, it should be more realistic to rather invoke the representativeness error, even at a close range. Nevertheless, the slopes of linear regressions, close to unity, express some satisfying agreement in average.

The opposite, i.e., worst performances for X-band radar in terms of slopes in spite of quite good correlation values, is observed in the case of the December 2–3, 2006 event (Fig. 6). Here the statistical criteria show a better coherence between the S-band and the gauge results (with a slope of 0.98), in opposition to those observed between the X-band radar and the gauge figures (with a slope of 0.81).

These results are very close to those obtained within the 0–30 km range. This could be due to some important statistical weight assigned to the 0–10 km area (2/3 of the whole sample gathered was considered in the 0–30 km area). However, this is statistically compensated by the strong rain intensities observed only beyond the 10-km range.

4.3. Rainfall intensity threshold

The distribution of rain from gauge measurements showed that most of the events were highly dominated by the low rainfall rates. Further analyses were thus carried out to check the influence of this large number of low rainfalls on the overall statistics. For this purpose, the radar-gauge comparison plots were set up according to various ranges of rainfall intensities (Fig. 9).

Comparing columns 1 and 2 of Table 8 (respectively including and not including the zero values registered by gauges while being registered as nonzero values by the radar), we can observe that the difference between the two data sets has a negligible impact on the statistics, even when the number of samples is reduced by 2. The statistical results are less satisfactory with higher intensity ranges, especially with the gauge rain rates greater than 3 mm/h (with Nash criterion >−0.15). The number of points (<390), which is about ten times smaller than in the first column (3256), may certainly contribute to the smaller correlation values. In contrast with the determination coefficient and the Nash criterion, the slopes of the linear regression are not altered when the intensity range increases. However, for the gauge rain rates greater than 5 mm/h the intercept values are found to be greater than 1 mm/h for both, radar vs. gauge comparisons.

Table 8
Statistical criteria for different ranges of rainfall rates based on the combined gauges data on all events within a range of 0–60 km. Rg denotes the rain gauge measurements. The various statistical criteria presented in this table are explained in Table 4.

Rain gage threshold	⩾0 mm/h	>0 mm/h	>1 mm/h	>3 mm/h	>5 mm/h
Nash GX	0.79	0.78	0.72	0.62	0.55
Nash GS	0.76	0.74	0.67	0.54	0.41
Nash SX	0.71	0.67	0.53	0.38	0.26
R^2 GX	0.80	0.79	0.74	0.68	0.64
R^2 GS	0.76	0.75	0.69	0.61	0.56
R^2 SX	0.74	0.72	0.62	0.52	0.43
Slope GX	0.94	0.92	0.92	0.94	0.96
Slope GS	0.91	0.86	0.82	0.83	0.88
Offset GX (mm/h)	−0.16	−0.23	−0.27	−0.70	−1.25
Offset GS (mm/h)	0.09	0.17	0.14	−0.16	−1.09
Number of points ⩾ 0 mm	3256	1464	765	390	233

5. Discussion and conclusion

The aim of this study was to assess the ability of a dual polarized X-band radar to estimate rainfall. The analysis was conducted by comparing X-band radar rain products with co-located S-band radar rain products and rain gauge data.

The dual polarized X-band radar (Hydrix® designed by Novimet) is associated with the ZPHI® algorithm to correct attenuation and to estimate the rainfall rate. The S-band radar (operated by Météo France) is located at only a 4-km range from the X-band radar. The two radars have similar scanning strategies (with multiple elevations), revisit times (2.5 min and 5 min) and beam apertures (1.5° and 1.2°). The main differences are the reflectivity attenuation, which is negligible at S-band and the rain algorithm. Indeed, the S-band radar derived rain estimation is corrected in real time with rain gauge data.

This study was carried out on the "Réal Collobrier" catchment area, in south of France, during autumn 2006. Four rainfall events

characteristic of the Mediterranean climate are analysed, considering different accumulation times (from 5 min to 6 h), different distances from the radar and different rainfall intensities. Within a 60-km range from the radars, the X-band and S-band radar derived 1-h rain products were in good agreement with the rain gauge measurements as shown by a Nash of 0.79 and 0.76, respectively. In the dataset, a large number of the rainfall values corresponds to low rainfall rates (<1 mm/h) and therefore may affect the statistical results. Nevertheless, it turned out that the results were not influenced by the lower rain gauge rates (<1 mm/h).

The rainfall rates estimated using the two radars were relatively close to rain gauge measurements. The X-band and S-band radar derived rain products were generally slightly lower than the rain gauge values, as shown by a slope of 0.94 and 0.91, respectively. Smith [26] also reported that radars underestimated the rainfall in comparison with ground gauge methods. These underestimates are relatively more important when the measurements are carried out far from the radar. It emerges from this study that results derived from S-band and X-band radars are not bias-free. The analysis of the hourly rainfall accumulation showed differences between the studied events. For example, during the December 02–03, 2006 event, the X-band radar derived rainfall estimation presented a larger bias compared to the gauge data, possibly due to an inappropriate calibration.

The closest area around the radars was the "Réal Collobrier" catchments, with Nash criteria of about 0.78 with the X-band radar and 0.76 with the S-band radar. The results obtained on the various distances from the radars are fairly coherent, but some variability in the outcomes was observed from one event to another. For the X-band radar, the Nash criteria were similar among the three areas studied with a variation of only 0.02 (Table 9). For the S-band radar, the same Nash criteria were obtained, mainly because, in opposition to the X-band radar results, the data obtained with the S-band radar were readjusted to the rain gauge data. The regression slopes slightly decreased as the distance increased (−0.03 with the X-band radar and −0.10 with the S-band radar).

Up to a distance of 60 km from the radar, it appeared that the performances of the X-band radar were quite stable and slightly better than the S-band ones in average. The beam broadening, beam height or inhomogeneous beam filling do not appears to influence much the performances. However, beyond 60 km, significant representativeness errors were noted (kept in mind that the bright band may contaminate more frequently the lowest scanning elevation angle).

In conclusion, in order to finalise our scientific assessment on the pertinence of a dual polarized X-band radar to estimate rainfall, we believe that further studies must be carried out in other experimental areas. Since June 2007, the X-band radar has been set up near Nice (Mont-Vial summit). The main difference between this site and the previous one is the lack of S-band radar data over this area. The X-band radar is intended to provide inputs to hydrological models. A relevant resolution for small urban catchments in Mediterranean regions requires very dense rain gauge networks [5]. The dual polarized X-band radar associated with ZPHI® does not require "on-line" calibration with gauges, which makes it a useful instrument for working in areas lacking rain gauge networks.

Next time, we shall discuss the advantages of combining X-band radar methods with a hydrological model, more specifically in terms of flood forecasting quality, as the potential of radar rainfall measurements for flood forecasting purposes is about to be put in practice in a very near future.

Table 9
Statistical criteria for hourly comparisons including all events within a distance of 10, 30, and 60 km from the radars. The statistical criteria presented in this table are explained in Table 4.

Distance to radar	0–10 km	0–30 km	0–60 km
Nash GX	0.78	0.80	0.79
Nash GS	0.76	0.76	0.76
Nash SX	0.77	0.78	0.71
R^2 GX	0.80	0.82	0.80
R^2 GS	0.78	0.77	0.76
R^2 SX	0.80	0.80	0.74
Slope GX	0.97	0.96	0.94
Slope GS	1.01	1.00	0.91
Number of points $\geqslant$ 0 mm	1276	1870	3256

Acknowledgements

FRAMEA is a European Intereg IIIA project between the Piemont Region (Italy), CETP (CNRS, Velizy), Météo France and Cemagref. This project has been supported by the following French institutions: Direction de l'Eau du Ministère de l'Ecologie et du Développement Durable, Conseil régional Provence Alpes Côtes d'Azur and Conseil Général des Alpes Maritimes.

The authors would like to thank Witold F. Krajewski and the three anonymous reviewers for their comments that considerably helped to improve this paper.

References

[1] Anagnostou MN, Anagnostou EN, Vivekanandan J, Ogden FL. Comparison of raindrop size distribution estimates, from X-band and S-band radar polarimetric observations. IEEE Geosci Remote Sens Lett 2007;4(4):601–5.
[2] Andrieu H, Creutin JD, Delrieu G, Faure D. Use of a weather radar for the hydrology of a mountains area Part I: radar measurement interpretation. J Hydrol 1995;193:1–25.
[3] Berenguer M, Corral C, Sanchez-Diezma R, Sempere-Torres D. Hydrological validation of a radar-based nowcasting technique. J Hydrometeorol 2005;6:532–48.
[4] Berne A, Delrieu G, Andrieu H. Estimating the vertical structure of intense Mediterranean precipitation using two X-band weather radar systems. J Atmos Ocean Technol 2005;22:1656–75.
[5] Berne A, Delrieu G, Creutin JD, Obled C. Temporal and spatial resolution of rainfall measurements required for urban hydrology. J Hydrol 2004;299:166–79.
[6] Borga M. Accuracy of radar estimates for streamflow simulation. J Hydrol 2002;267:26–39.
[7] Brandes EA, Vivekanandan J, Wilson JW. A comparison of reflectivity estimates of rainfall from collocated radars. J Atmos Ocean Technol 1999;16:1264–72.
[8] Ciach GJ. Local random errors in tipping bucket rain gauge measurements. J Atmos Ocean Technol 2002;20:752–9.
[9] Ciach GJ, Krajewski WF. On the estimation of rainfall error variance. Adv Water Res 1999;22:585–95.
[10] Ciach GJ, Krajewski WF. Radar-rain gauge comparison under observational uncertainties. J Appl Meteorol 1999;38:1519–25.
[11] Collier CG. Application of weather radar systems. Chickerster, UK: Ellis Horood; 1989.
[12] Delrieu G, Ducrocq V, Gaume E, Nicol J, Payrastre O, Yates E, et al. The catastrophic flash-flood event of 8–9 September 2002 in the Gard region France: a first case study for the Cévennes-Vivarais Mediterranean hydrometeorological observatory. J Hydrometeorol 2005;6:34–52.
[13] Delrieu G, Serrar S, Guardo E, Creutin JD. Rain measurement in hilly terrain with X-band radar systems: accuracy of path-integrated attenuation estimates derived from mountain return. J Atmos Ocean Technol 1998;16:405–16.
[14] Delrieu G, Hucke L, Creutin JD. Attenuation in rain for X-band and C-band weather radar systems: sensitivity with respect to the drop size distribution. J Appl Meteorol 1998;38:57–68.
[15] Einfalt T, Maul-Kötter B, Spies S. A radar data quality control scheme used in hydrology. Phys Chem Earth 2000;25(10–12):1141–6.
[16] Faure D, Delrieu G, Tabary P, Parent Du Chatelet J, Guimera M. Application of the hydrologic visibility concept to estimate rainfall measurement quality of two planned weather radars. Atmos Res 2005;77(1–4):232–46.
[17] Kirstetter PE, Delrieu G, Boudevillain V, Berne A. Toward an error model for radar quantitative precipitation estimation in the Cévènnes-Vivarais region, France. In: Fourth European conference on radar in meteorology and hydrology, Barcelona.
[18] Habib E, Ciach GJ, Krajewski WF. A method for filtering out raingage representativeness errors from the verification distribution of radar and raingauge rainfall. Adv Water Res 2004;27:967–80.
[19] Habib E, Krajewski WF. Uncertainty analysis of the TRMM ground validation radar rainfall products application to the Teflun-B field campaign. J Appl Meteorol 2002;41:558–72.

[20] Johnson D, Smith M, Koren V, Finnerty B. Comparing mean area precipitation estimates from NEXRAD and rain gauge networks. J Hydrol Eng ASCE 1999; 4(2):117–24.
[21] Krajewski WF, Smith JA. Radar hydrology: rainfall estimation. Adv Water Res 2002;25:1387–94.
[22] Le Bouar E, Moreau E, Testud J. The rain accumulation product from the X-band polarimetric radar HYDRIX, Weather radar and hydrology (WRaH2008), March 10–12, Grenoble, France, <http://www.wrah-2008.com/>; 2008.
[23] Le Bouar E, Testud J, Keenan TD. Validation of rain profiling algorithm ZPHI from C-band polarimetric weather radar, Darwin. J Atmos Ocean Technol 2001;18:1819–37.
[24] Parent du Chatelet J, Tabary P, Gueguen C, Fradon B. The Météo France single-radar and composite QPE operational products. In: Fourth European conference on radar in meteorology and hydrology, Barcelona; 2006.
[25] Rivrain JC. Les épisodes orageux à précipitations extrêmes dans les régions méditerranéennes du Sud de la France, Phénomènes remarquables vol. 4, Météo France, SCEM; 1998. 93 pp.
[26] Smith AJ, Seo DJ, Baeck ML, Hudlow MD. An intercomparison study of NEXRAD precipitation estimates. Water Resour Res 1996;32:2035–45.
[27] Sun X, Mein RG, Keanan TD, Elliott SF. Flood estimation using radar and raingauge data. J Hydrol 2000;239:4–18.
[28] Tabary P. Using radars for rainfall estimation: the point of view of an operational service, Weather radar and hydrology (WRaH2008), March 10–12, Grenoble, France, <http://www.wrah-2008.com/>; 2008.
[29] Testud J, LeBouar E, Obligis E, Ali-Mehenni M. The rain profiling algorithm applied to polarimetric weather radar. J Atmos Ocean Technol 2000;17: 332–56.
[30] Uijlenhoet R, Stricker JNM, Russchenberg HWJ. Application of X- and S-band radars for rain rate estimation over an urban area. Phys Chem Earth 1997;22(3–4):259–64.
[31] Wang D, Smith MB, Zhang Z, Reed S, Koren V. Statistical comparison of mean area precipitation estimate from WSR-88D operational and historical gage networks, paper 2.17. In: 15th conference on hydrology, January 9–14, Long Beach, CA: American Meteorological Society; 2000.
[32] Wilson JW, Brandes EA. Radar rainfall measurement: a summary. AMS Bull 1979;60:1048–58.
[33] Zawadzki I. Factors affecting the precision of radar measurements of rain, Preprints. In: 22nd conference radar meteorology. Zurich: Am. Meteorol. Soc.; 1984. p. 251–6.